

Cite this: DOI: 10.1039/c1ee01913a

www.rsc.org/ees

PERSPECTIVE

Membrane-based production of salinity-gradient power

Guy Z. Ramon, Benjamin J. Feinberg and Eric M. V. Hoek*

Received 8th June 2011, Accepted 13th July 2011

DOI: 10.1039/c1ee01913a

This perspective paper outlines the fundamental principles and state-of-the-art of membrane-based conversion of salinity-gradient energy, a renewable and environmentally benign energy source receiving increased attention in recent years. In particular, an attempt is made to identify the most important and promising directions for future research and technological innovation.

Introduction

The need for renewable, environmentally benign energy is widely recognized, and hence, massive efforts are being exerted globally to develop new 'green energy' sources including: wind, solar, geothermal, biomass, ocean thermal, wave, and tidal. Perhaps less well known is salinity-gradient energy, which is the energy available from mixing two aqueous solutions of different salinities. Referring to the fact that the chemical potential difference between ocean water and river water is equivalent to ~ 270 m of hydraulic head, river mouths have been termed 'silent waterfalls'. Salinity gradient energy has been estimated to be the second largest marine-based energy source, with a total estimated global potential for power production placed at 1.4–2.6 TW.^{1,2} These values are comparable with the total electricity currently produced worldwide; for comparison, in 2007, the electricity production from hydro-electric sources was estimated to be 0.8 TW.³ The reported estimates for salinity-gradient power account for production through the mixing of all major river outfalls with seawater around the world; as such, it is highly unlikely that its potential will ever be fully realized. A recent study has placed the total global potential at ~ 1.9 TW;⁴ furthermore, it was estimated that, considering technical issues relevant to actual energy

conversion (*e.g.*, percent recovery, averaged river flow-rates, source salinities and temperatures) 60% of this energy would be available for extraction, or ~ 980 GW (see Table 1 for estimated values of salinity-gradient sources). This is still a significant amount of renewable power; however, it is likely to be further reduced due to local considerations such as size, site compatibility, and regulatory constraints which may also include consideration of environmental impacts on the estuaries. Nevertheless, potential exploitation of major river mouths is actively being sought; 2009 saw the first demonstration of salinity-gradient power plant becoming operational in Norway, with a projected capacity of 10 kW,⁶ while a 25 MW installation is expected to become operational in 2015.

Another potential dilute stream, not included in this estimate, is non-reused municipal wastewater effluent. The total potential

Table 1 Potential power production from some salinity-gradient sources

Energy source	Power (GW)
River- Seawater, global	983 ^a
Zaire	57 ^a
Ganges	25 ^a
Mississippi	18 ^a
Rhine	2 ^a
Wastewater, global	18.5 ^b

^a ref. 4 ^b Estimated based on data from ref. 5

Department of Civil & Environmental Engineering and California NanoSystems Institute, University of California, Los Angeles, CA, 90095-1593. E-mail: emvhoek@ucla.edu; Tel: +(310) 206-3735

Broader context

When two streams of different concentrations are mixed, energy is released. This energy may be converted into useful electricity through the controlled mixing of two streams of varying salinity; for example, recent assessments have placed the potential power which may technically be converted from the mixing of seawater and river water at ~ 1 TW. Controlled mixing is the main challenge in harnessing this form of energy and may be achieved by the use of membranes, which act as semi-permeable barriers, thus enabling the preferential transport of either water (osmosis) or ions. These two modes of membrane-based mixing are currently being developed intensively, the primary goal being the design and fabrication of efficient membranes. This perspective paper provides an overview of these two techniques, their theoretical framework and state-of-the-art; in particular, the most important characteristics are emphasized and potential avenues for improvements are identified.

global power production from wastewater discharged into the sea is estimated as ~ 18.5 GW, which is comparable with the power available from the average discharge of the Mississippi river (note: there is ~ 65 MW capacity in Southern California alone). A number of possible scenarios may be considered using municipal wastewater effluent as the fresh water source. The brine from nearby brackish or ocean water desalination plants may be controllably re-mixed with wastewater effluents prior to discharge; thus, recovering some of the energy invested in the desalination processes. All these, however, depend on the technological capacity to efficiently and cheaply extract this form of energy.

When two aqueous solutions of different salinity are brought in contact, they will spontaneously mix; this is the driving force for the mixing process. The difference in free energy upon mixing of two solutions is the sum of the chemical potentials of the original, unmixed solutions minus the chemical potential of the final mixture. For a NaCl solution under constant pressure and temperature, the free energy of mixing may be written as

$$\Delta E_{mix} = 2R_g T \left(c_c \ln \frac{c_c(1+\varphi)}{c_c + \varphi c_d} + \varphi c_d \ln \frac{c_d(1+\varphi)}{c_c + \varphi c_d} \right) \quad (1)$$

where R_g is the universal gas constant, T the absolute temperature, c_d and c_c are the solute concentrations in the dilute and concentrated solutions, respectively, and $\varphi = \frac{V_d}{V_c}$ is the dilution ratio, with V the volume of the solutions being mixed. As an order of magnitude estimate - mixing equal volumes (1 m^3) of seawater ($\sim 0.5 \text{ M}$) and a fresh river water ($\sim 5 \text{ mM}$) releases ~ 0.5 kWh of energy, the hydroelectric equivalent of which being 1 m^3 of water flowing down a 175 m waterfall. The concentrated solution may be regarded as the energy source here and the more it is diluted, the more energy is extracted; on the other hand, the energy density of the process is largest at the initial, undiluted salinity gradient. This is illustrated in Fig. 1, where the energy extracted from 1 m^3 of seawater is plotted as a function of the dilution ratio (with an increasing volume of fresh water), along with the scaled energy density (*i.e.*, the energy density at the given dilution divided by that available at the initial concentration). The competing effects of these two metrics are clearly apparent and, in the idealized case presented, an optimum compromise exists when mixing equal volumes. However, the calculation

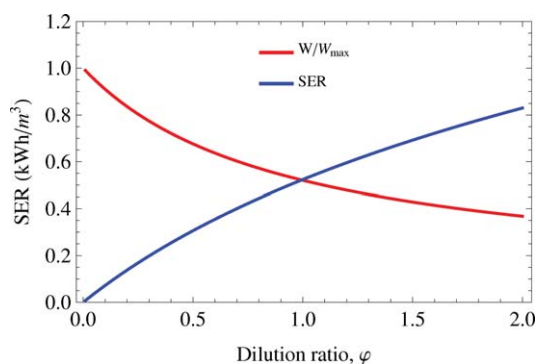


Fig. 1 Specific energy recovery (SER) and the scaled power density (W/W_{max}), plotted against the dilution ratio, *i.e.*, the volume of dilute solution per unit volume (m^3) of concentrated solution.

performed here is merely illustrative of the approach, which should be employed with greater computational rigor in future optimization of the process.

While several methods exist for the extraction of salinity-gradient energy, the focus of this paper is on membrane-based techniques. Two such technologies currently exist: pressure-retarded osmosis (PRO) and reverse electro-dialysis (RED), both of which are theoretically opposite versions of two technically and commercially mature membrane separation processes: reverse osmosis (RO) and electro-dialysis (ED), respectively. In the following sections, the fundamental principles of these technologies and their current state-of-the-art will be presented, followed by an analysis of their projected potentials. In particular, we attempt to identify the most promising routes for improvement over the state-of-the-art by defining the most important parameters affecting process performance.

Fundamentals of PRO and RED

Pressure-retarded osmosis

The operating principle of PRO is simple; driven by the chemical potential difference, water diffuses through a semi-permeable membrane from a low salinity stream (high chemical potential) into a high-salinity (low chemical potential), pressurized stream; thereby, increasing its pressure and flow rate.^{7,8} The augmented flow of the pressurized stream then passes through a hydroelectric turbine which extracts the power (Fig. 2). The driving force for osmosis is the water chemical potential gradient across the membrane which, in an isothermal system, may be expressed as the difference in osmotic pressure of the concentrated and dilute solutions. Accounting for the applied hydraulic pressure, which diminishes this driving force, the resulting 'pressure-retarded' osmotic water flux may be expressed as

$$J_w = A(\Delta\pi - \Delta P), \quad (2)$$

where A denotes the membrane water permeability, ΔP the hydraulic pressure drop across the membrane and $\Delta\pi$ is the osmotic pressure difference across the membrane.

The power in a PRO process is completely analogous to hydroelectric power and is the product of the augmented flow rate and pressure drop through a hydro-turbine. The power density (per unit membrane area) for a PRO process is therefore

$$W = J_w \Delta P = A(\Delta\pi - \Delta P)\Delta P \quad (3)$$

For example, if the concentrated stream is pressurized to ~ 10 bar ($\sim 1 \text{ MPa}$), then for a permeation flow rate of $1 \text{ m}^3/\text{s}$ the power output would be ~ 1 MW. Furthermore, it is straightforward to show that the maximum power density occurs when the applied pressure is equal to half the osmotic pressure by taking the derivative of eqn (3) with respect to ΔP and equating to zero, resulting in the following equation for the maximum power density:

$$W_{max} = \frac{A}{4} \Delta\pi^2 \quad (4)$$

It is immediately obvious from eqn (4) that the prerequisite for an efficient PRO process is the membrane permeability; a low

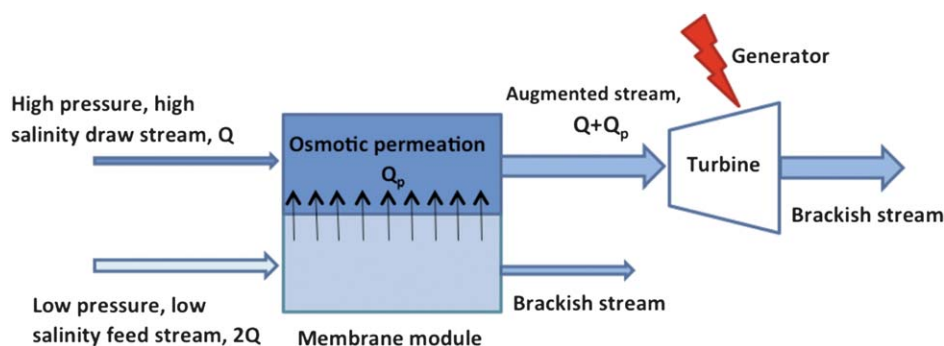


Fig. 2 Schematic drawing illustrating the pressure-retarded osmosis process. Water permeates through a selective membrane from a dilute stream (fresh water) into a pressurized concentrated stream (seawater), and is then expanded through a hydro-turbine.

permeability membrane would render the conversion of even a high salinity gradient hopelessly inefficient.

Mass transfer limitations in PRO

A second observation which follows from eqn (4) is that the maximum power density for a given membrane permeability occurs when the available concentration gradient is fully utilized, that is, when $\Delta\pi = 2R_gT(c_{b,c} - c_{b,d})$, where the subscript b denotes a bulk solution property. However, as with any other membrane-based process, performance is limited by concentration polarization (CP), which reflects the variation in concentration between the membrane surface and the bulk solution. However, polarization phenomena in PRO take on a somewhat different, more complex form, compared with traditional RO processes. Osmotic permeation from the dilute stream into the concentrated stream causes its dilution at the membrane surface and is referred to as 'dilutive external CP'. This type of polarization is the opposite of that encountered in RO membrane separations but may, in principle, be similarly minimized through enhancement of mass transfer external to the membrane. On the other side of the membrane (the dilute side), salt is rejected and accumulates in a completely analogous manner, except that the porous media like character of modern RO membrane supports comes into play.

Most modern salt rejecting (RO-like) membranes are composed of a very thin (~ 100 nm) dense film over a porous structure, which offers mechanical support. This asymmetric structure, particularly the porous support, results in an additional resistance to mass transfer which has been termed 'internal CP'.^{9,10} Internal CP is caused by two mechanisms (Fig. 3): the first is the rejection and subsequent accumulation of salt present in the dilute stream, and the second is diffusive salt diffusion through the membrane (which is always present, even for highly rejecting membranes) driven by the concentration gradient from the concentrated to the dilute side. This 'salt leakage' is further exacerbated by the presence of water permeation in the opposite direction, which further contributes to salt accumulation within the support structure. The occurrence of internal CP results in a reduction of the available driving force for osmosis and may be regarded as an artificial source of inefficiency in PRO energy conversion due to the construction of modern RO membranes.

Using a simplified theoretical approach based on film theory, it has been shown that the 'effective' osmotic pressure difference

across the membrane during PRO operation, accounting for the effects of internal and external CP, may be written as^{10,11}

$$\begin{aligned} \Delta\pi &= 2R_gT(c_{m,c} - c_{m,d}) \\ &= 2R_gT \left(\frac{c_{b,c} \exp\left(\frac{-j_w}{k}\right) - c_{b,d} \exp\left(\frac{j_w S}{D}\right)}{1 + \frac{B}{j_w} \left(\exp\left(\frac{j_w S}{D}\right) - 1 \right)} \right). \end{aligned} \quad (5)$$

Here, B denotes the salt permeability coefficient, an intrinsic membrane property, k is the mass transfer coefficient and S is the structure factor for the porous support, defined as

$$S = \frac{\tau\delta}{\varepsilon}, \quad (6)$$

where τ , ε and δ are the tortuosity, porosity, and thickness of the support structure, respectively. The structure factor may be interpreted as the 'effective' membrane thickness for diffusive transport. An ideal membrane would have a structure factor of zero, which would produce no internal CP; this is at present an unattainable idealization given the limits of materials science. Therefore, reduction of the support layer mass transfer resistance is sought. In fact, minimization of internal CP was already targeted by early PRO research as a limiting factor for its potential commercialization and has remained the focus of most efforts for development of suitable membranes for PRO energy conversion.⁹

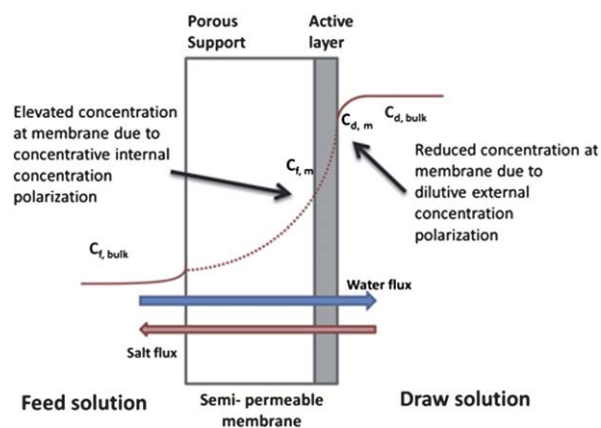


Fig. 3 Schematic drawing illustrating internal and external concentration polarization when an asymmetric membrane is used for pressure-retarded osmosis.

Within the film theory framework, the external mass transfer coefficient, k , is governed by the hydrodynamics of the channels on either side of the membrane. As such, it is strongly affected by the specific configuration used to pack the membranes. For the purpose of our foregoing analysis, a spacer-filled channel will be assumed, characteristic of commercially available spiral-wound RO modules. For such geometry, the following correlation, which is based on CFD simulations,¹² is used herein:

$$k = 0.46(ReSc)^{0.36} \frac{D}{d_h}, \quad (7)$$

in which d_h is the channel's hydraulic diameter, $Sc = \frac{\nu}{D}$ is the Schmidt number (on the order of 600–700 for seawater) and $Re = \frac{ud_h}{\nu}$ is the Reynolds number (on the order of 50–300 in commercial spiral-wound modules), where u is the mean velocity in the channel and ν is the fluid's kinematic viscosity.

Other losses

The theoretical description of power production in PRO, as presented by eqn (3) with eqn (5) used for calculating the effective osmotic pressure, does not consider several additional power losses, which may be present in practice. These include turbine efficiency and pumping power requirements. For the latter, hydraulic energy recovery devices may be employed so that losses are, for the most part, expected to result from dissipation within the membrane module. This important aspect must be carefully considered in conjunction with any attempt at increasing the feed velocity for mass transfer enhancement; clearly, such enhancement comes at an energetic penalty which may outweigh its merit in terms of net power production. The assumption that the feed streams are pure electrolyte solutions is clearly an idealization; in practice, the feed streams contain organic matter, colloidal particles, bacteria and other impurities. These may incur additional losses through fouling/bio-fouling and, in particular, clogging of the porous support through which water flows from the dilute side. Lastly, the axial variation of concentrations and pressures on either side of the membrane results in a reduced driving force as well as deviation from the 'optimum' applied pressure, which is likely to be an averaged value. Prediction of these aspects requires a more rigorous model than is used herein and, indeed, is currently available in the literature.

Reverse electrodialysis

Reverse electrodialysis was developed using stack design, membranes, and system parameters available from the electrodialysis process, operated in reverse. In this case ion selective membranes separate relatively diluted (*e.g.*, river water) and concentrated (*e.g.*, seawater) solutions. However, unlike electrodialysis where an applied voltage induces ion migration, in RED the driving force is a concentration difference between the feed streams which produces an electrochemical potential gradient. Driven by the concentration difference, cations and anions diffuse across membranes with opposing-charge functional groups, creating an ionic flux. A full-scale RED system is composed of multiple cell pairs, each consisting of a dilute feed channel, concentrate feed channel, and corresponding anion/

cation exchange membranes; this membrane 'stack' terminates with electrodes at each end, which convert the ionic flux into an electric current through oxidation-reduction reactions (Fig. 4).

Unlike PRO, RED is an electro-chemical process which converts the ionic flux directly into electric current. The power produced is related to the electro-chemical potential drop across the membrane, ΔV , and an external load resistance, resulting in¹³

$$W = I^2 R_{load} = \frac{\Delta V^2 R_{load}}{(R_{stack} + R_{load})^2} \quad (8)$$

where R_{load} is the load resistance. The potential across the membrane is related to the concentration difference *via* the Nernst equation,

$$\Delta V = 2 \frac{\alpha R_g T}{F} \ln \frac{c_c}{c_d} \quad (9)$$

in which F is the Faraday constant and α is the permselectivity, a measure of the membrane's ability to transport a specific charge-carrier, *i.e.*, cations or anions. The stack resistance,

$$R_{stack} = R_{aem} + R_{cem} + \frac{h_c}{\kappa_c} + \frac{h_d}{\kappa_d} + R_{electrode} \quad (10)$$

is the sum of the anion exchange membrane resistance, R_{aem} , the cation exchange membrane resistance, R_{cem} , the two channel resistances where h_d is the dilute feed channel height, h_c is the concentrated feed channel height, κ_c the concentrated feed conductivity, and κ_d the dilute feed conductivity. The electrode resistance, $R_{electrode}$, is assumed to be negligible for a stack containing a large number of cell pairs. As with PRO, it may be shown that the maximum power density occurs when the external load resistance is matched with the membrane potential,

$$W_{max} = \frac{1}{2R_{stack}} \frac{\Delta V^2}{4} \quad (11)$$

It is apparent that both processes are controlled by the effective driving force and the ability of the system to transmit the desired species required for power conversion.

Process losses

As with any other membrane process, concentration polarization is inherently present for RED, albeit predominantly in a purely diffusive form, since convection due to osmosis is very weak. Concentration polarization results in a decreased electrochemical potential gradient across the membrane. In order to account for this possible change in the membrane surface concentration, the following expression may be used to relate the bulk and membrane concentrations:

$$C_m = C_b \pm \frac{J}{k} \quad (12)$$

where $J = \frac{I}{F}$ is the mass flux of ions. Eqn (12) thus reflects the increase/decrease of the membrane surface concentration at the dilute/concentrated solution-membrane interface. Losses from co-ion transport and electro-osmosis are most significant at low current densities. At higher current densities these effects have been shown to be negligible.¹⁴

An important loss in RED systems is that due to spacers used in order to mechanically support the flow-channels when membranes

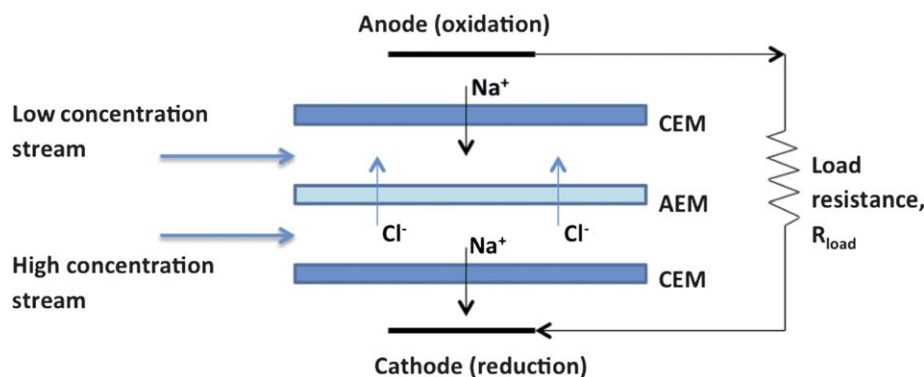


Fig. 4 Schematic drawing of a reverse-electrodialysis cell, illustrating the alternating feed channels and membranes, as well as the external electric circuit used to extract the power.

are stacked together. As with PRO, viscous dissipation is also present in RED and may be exacerbated by the presence of spacers. Moreover, spacer material and geometry can have a significant impact on the efficiency of an RED process through interference with ionic transport and changes in the effective membrane surface area. It has been demonstrated that this “shadow effect” can reduce process efficiency by up to 40%.¹⁵ In order to minimize the shadow effect, Dlugolecki *et al.* replaced the traditional spacers with conductive spacers (cut out of ion-exchange membranes) containing an anion-conducting part and a cation-conducting part.¹⁶ Conductive spacers significantly reduced stack resistance and increased power density by three to four-fold.

Electrode performance is another consideration in RED stack design; however, electrode losses are considered to be much less contributory to overall stack resistance than membrane resistance, compartment height, and other factors. Experiments have shown that electrode losses scale inversely with stack size.¹⁷ Veerman *et al.* determined that segmented electrodes increase total power output in RED systems.¹⁸ The authors hypothesized that the lower the stack residence time, and thus, the lower the concentration difference between flow inlet and outlet, the less the influence of electrode segmentation on total power output.

Most RED experiments reported in the literature have used pure electrolyte solutions for the concentrated and dilute solution feeds to demonstrate that power can be generated. While using pure solutions simplifies experiments it does not adequately simulate real world multi-component electrolytes. Post *et al.* investigated the impact of multivalent ions on the power density generated from an RED stack. The presence of multivalent ions contributed to increased stack resistance and decreased stack voltage.¹⁹ The authors found that multivalent ions were diffusing from the dilute solution to the concentrated solution against the electrochemical potential gradient. In order to prevent the transport of multivalent ions across the membranes, the use of monovalent-selective membranes was suggested.

Current state-of-the-art

Pressure-retarded osmosis

Work on PRO dates back to the 1970's^{7,8} but has seen significant progress in the past few years, primarily through the development of better membranes. It is important to note that no actual

power has ever been produced in any known PRO studies reported in the literature; rather, a measured permeation rate at the experimentally applied pressure is converted to power using eqn (3). Experimental work has been thus far mostly limited to lab-scale testing of commercially available RO and FO membranes,^{9–11,20–21} or prototype lab-cast membranes.^{22–26} Recently, experiments have been reported where commercial FO spiral-wound modules were used.²⁷ The maximum power densities reported in the literature as inferred from experimental measurements, using seawater-equivalent as the concentrated stream, are ~ 0.5 W/m² in a commercially available spiral-wound module (Hydrowell, Hydration Technology Innovations Inc., Albany, Oregon, USA),²⁷ 2.7 W/m² with the same commercial membrane lab-tested,¹¹ and 3.5 W/m² with a prototype, lab-cast TFC membrane.²²

There has been significant progress made recently in the fabrication of FO membranes. While these were not specifically tested for PRO operation (*e.g.*, permeation rates under pressurized conditions), their estimated potential performance may be calculated based on the experimentally determined characteristics, namely, the water and salt permeabilities and the structure factor of the support. Table 2 provides a compilation of FO membranes, their reported characteristics and projected power densities, calculated using eqn (4) and (5). Power calculations were made assuming the concentrated solution is either seawater or seawater RO brine after 50% recovery (0.55 M and 1.1 M as NaCl, respectively) and that the dilute stream has a concentration of 0.005 M, representative of river water, or 0.02 M, representative of waste-water, and the Reynolds number was taken to be 100, which may be considered as a representative value for operation of spiral-wound membrane modules.

The membrane with the best structure factor reported thus far is a cellulose-acetate phase-inversion membrane with a thickness of $\sim 35\mu\text{m}$ and a structure factor of $\sim 50\mu\text{m}$,²⁵ followed by $\sim 310\mu\text{m}$ reported for a thin-film composite polyamide/poly-sulphone membrane,²⁶ which along with its relatively high permeability ($\sim 5.3 \times 10^{-12}$ m/s·Pa) has the highest projected performance at 6.1 W/m² and 15.3 W/m² for seawater and RO brine, respectively, serving as the concentrated solution. The highest reported permeability is $\sim 7 \times 10^{-12}$ m/s·Pa,²² also for a composite membrane, which is about double that of the average commercial seawater RO membrane. The current generation of prototype membranes, particularly those recently

Table 2 Characteristics of commercial and prototype osmotic membranes and their potential power density

Membranes	Water Permeability $\times 10^{-12}$ m/Pa•s	Salt Permeability $\times 10^{-7}$ m/s	Structure factor μm	Power density (W/m^2)	
				Seawater	RO Brine ^b
Lab Cellulose-Acetate-FO ²⁵	0.41	0.22	52	0.7	2.7
Lab TFC-FO ²⁶	5.27	0.91	312	6.1	15.3
Lab TFC-FO ²⁴	3.22	1.3	492	3.8	10.1
Lab TFC-FO (hollow fiber) ²³	6.2	0.56	595	5.5	8.7
Commercial FO Cellulose Tri-Acetate ^{11,24}	2.2	1.2	625	2.8	7.8
Lab TFC-FO ²²	7.1	1.1	670	4.7	6.5
Commercial RO Cellulose-Acetate ^{a24}	2	0.6	1000	2.4	5.9
Commercial TFC-RO ^{a24}	1.6	0.8	2200	1.2	2.1

^a without fabric support. ^b Dilute stream concentration 0.02M, representative of wastewater.

reported by Tiraferi *et al.*,²⁶ already achieve the ~ 5 W/m^2 power density which has been flagged as the target for making PRO economically viable.²⁸ That being said, this power density is idealized and is expected to be significantly lower in practice, primarily due to dilution effects and hydraulic losses, as previously discussed. It is particularly curious to note the lack of a definitive correlation between the structure factor and estimated power output; this will be discussed further in the following section.

An important characteristic of any PRO membrane is its ability to withstand the applied hydraulic pressure in the feed stream. Since a maximum power output is achieved when this applied pressure is about half the osmotic pressure, it follows that the higher the concentration difference (larger energy source), the higher the necessary applied pressure for power maximization. For example, when RO brine (1.1M, twice the concentration of seawater) is contacted with 0.02M wastewater, the optimum applied pressure would be ~ 24 bar. It is not clear whether the currently available membranes, as compiled in Table 2, would be able to mechanically withstand such an applied pressure

Reverse electro dialysis

Investigation into the use of RED as a salinity gradient energy technology emerged in the early 1950s when Pattle constructed a small stack that produced a maximum electromotive force of 3.1 Volts.²⁹ Due to the high internal resistance associated with the stack, power outputs were relatively low. This approach was further developed during the late 1970's, with the theoretical foundation laid down by Weinstein and Leitz¹³ and, later, by Lacy.³⁰ Ion exchange membranes have not been specifically designed for the RED process and research has been conducted using membranes developed for ED. The most important membrane properties are the permselectivity and electrical conductivity. A variety of commercially available cation and anion exchange membranes were studied by Dlugolecki *et al.*³¹ with the drawn conclusion that power density is more sensitive to changes in membrane conductivity than permselectivity. Recent advances in polymer and materials science have resulted in significant improvements to ion-exchange membranes.³² Table 3 lists the reported characteristics of a number of commercially-available ion-exchange membranes. Most of the commercially available membranes are homogenous, that is, fabricated solely

from the ion-exchange polymer. Lower performance, heterogeneous membranes are also available, to a much lesser extent; these are fabricated using mixed ratios of ion-exchange polymer with another, inert, polymeric carrier. While achieving permselectivity comparable with that of homogeneous membranes, heterogeneous membranes are 3–4 times less ion-conductive.

Veerman *et al.*¹⁴ benchmarked six cation-anion membrane pairs and found that the Fumasep (FAD and FKD) and Selemion (AMV and CMV) membrane combinations obtained the highest power density of approximately 1.2 W/m^2 . This power density was achieved for artificial river water and seawater with concentrations of 1 g/L and 30 g/L NaCl, respectively. As the membrane electrical conductivities/resistances were not published, it is difficult to compare the individual performance of these membranes to those in other studies. Commercial IEX membranes Neosepta CM-1 (cation exchange) and Selemion AFS (anion exchange) have been shown to have the lowest electrical area conductivities (reciprocal of the area resistance), measured to be $\sim 6,000$ and $\sim 15,000$ S/m^2 , respectively.³² An important part of the RED stack, electrode performance has been shown have a minor impact on stack resistance;¹⁷ therefore, further investigation into electrode materials is unlikely to result in significant power density improvements. Electrode segmentation is a novel concept which should certainly be incorporated into future large-scale optimization of RED stacks.³³ For the most part, RED stacks studied in the literature have been small-scale systems with limited membrane surface area and cell pairs. However, Veerman *et al.* recently developed a 50-cell RED stack in order to demonstrate the performance of a comparatively large system.¹⁸ This system was able to achieve a power density of 0.93 W/m^2 , the highest power density achieved in practice from a sea-river water salinity-gradient source.

Assessment of process potential

In what follows, calculations have been made with the purpose of illustrating the relative impact of various process characteristics on the overall performance in terms of the power density. Unless otherwise noted, the concentrated stream is sea water (represented by a 0.55M NaCl solution) and the dilute stream is river water (represented by a 0.005M NaCl solution). The calculated power should be considered the 'maximum power density' in the sense that the applied hydraulic pressure is taken to be half of the

Table 3 Characteristics of commercial ion-exchange membranes and their potential power density

Anion Exchange Membranes	Type	Permselectivity	Conductivity (10^4 S/m ²)	Power Density (W/m ²)
Neosepta AFN, ¹⁶	Homogenous	88.9	1.43	1.23–1.30
Selemion APS, ¹⁶	Homogenous	88.4	1.47	1.23–1.30
Fumasep FAD, ³¹	Homogenous	86	1.12	1.16–1.24
Neosepta AMX, ³¹	Homogenous	90.7	0.43	1.02–1.22
Ralex AMH-PES, ¹⁶	Heterogenous	89.3	0.13	0.73–1.12
Cation Exchange Membranes	Type	Permselectivity	Conductivity (10^4 S/m ²)	Power Density (W/m ²)
Neosepta CM-1, ³¹	Homogenous	97.2	0.60	1.12–1.30
Fumasep FKD, ¹⁶	Homogenous	89.5	0.47	0.99–1.19
Neosepta CMX, ³¹	Homogenous	99	0.34	1.02–1.30
Ralex CMH-PES, ¹⁶	Heterogenous	94.7	0.09	0.73–1.23

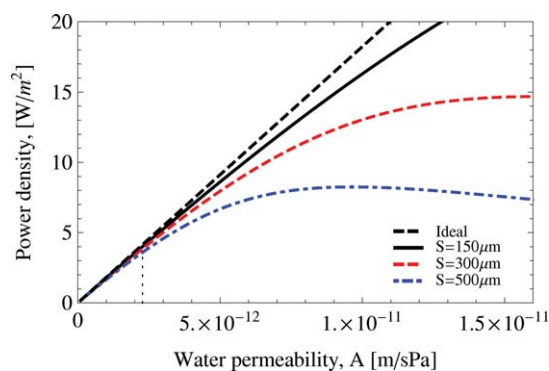


Fig. 5 Variation of PRO power density with increasing water permeability, for different values of the structure factor, S , under complete mixing conditions (no ECP). Also shown is an ideal power curve, calculated without any mass transfer limitations. The vertical dotted line marks the water permeability of a commercially available FO membrane. In these calculations, the salt permeability is set at $B = 10^{-7}$ m/s, the concentrated solution is seawater (0.55 M) and the dilute solution has a concentration of 5mM.

effective osmotic pressure (see eqn (4)), and the external load resistance is taken as half the effective membrane potential (see eqn (11)). Wherever present, the competing nature of the pertinent parameters is highlighted, with the goal of emphasizing future optimizations required for maximizing the potential for energy conversion. Notably, our analysis of PRO demonstrates that current membrane performance is limited by the water permeability and not by internal polarization, as is commonly assumed; moreover, a reduced salt selectivity, which may accompany improvements to the water permeability, may be tolerated to a large extent. Finally, the structure factor achievable by the current generation of membranes is a process limitation only when the 'dilute' stream has a high salinity, *e.g.* brackish water or higher, or if salt passage becomes excessively high. For RED, our analysis shows that relatively little improvement can be gained by increased membrane performance; furthermore, any such improvement must be accompanied by increased mass transfer. More specifically, the current generation of homogeneous membranes is already close to being optimal, while heterogeneous membranes may still be improved by reducing their electrical resistance, for example, by making

them thinner. In either case, the relative impact on the power density is not substantial.

Mass transfer limitations

We begin by examining the limitations imposed by mass transfer, *i.e.* external and, for PRO, internal concentration polarization. Recent efforts on improving membrane characteristics for PRO have focused their attention on the minimization of the support membrane structure factor. Assuming that there are no external mass transfer limitations, that is, complete mixing of the streams, Fig. 5 shows the variation of the power output with membrane water permeability for different structure factors. Note how, for the representative permeability of current FO membranes (marked with a vertical dotted line) changing the structure factor has a minor impact on the power density. Only upon a significant increase of the water permeability does the advantage of a smaller structure factor come into play, reach a maximum and then decline once again as internal polarization becomes a limiting factor. For the best prototype membrane permeability, a structure factor greater than 500 μm will limit performance. A similar trend is observed when the effect of external polarization is considered (Fig. 6), calculated with a structure factor of 50 μm , the lowest achieved so far; external mass transfer variations are manifested through the Reynolds number which embodies any changes made to the flow velocity or channel hydraulic diameter.

The power production is only weakly limited by external mass transfer; in fact, model calculations predict that for a low structure factor, the membrane permeability can be increased by nearly one order of magnitude before external mass transfer would limit the power density. It must be noted that, as already mentioned, any increase in the operating Reynolds number would also result in parasitic hydraulic losses which are not accounted for in the model used herein; such losses must be considered at the module-scale, as they may overwhelm any power gained by increased mass transfer.

The RED process is much less sensitive to mass transfer and membrane conductivity, since other resistances in the system, particularly the dilute channel resistance, play a dominant role in imposing the process limitation. Typical operating conditions reported in the literature are at a Reynolds number on the order of unity, two orders of magnitude lower than in PRO. Given

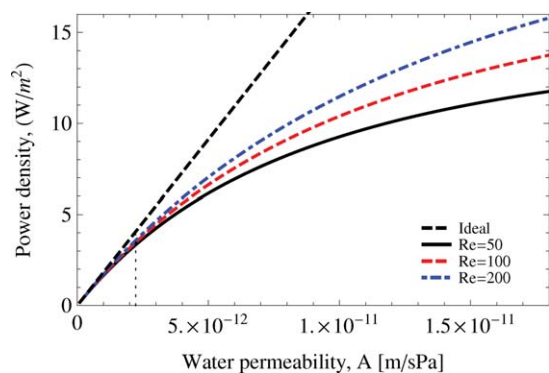


Fig. 6 Variation of PRO power density with increasing water permeability, for a membrane with $S = 50 \mu\text{m}$, showing the effect of external mixing. Also shown is an ideal power curve, calculated without any mass transfer limitations. The vertical dotted line marks the water permeability of a commercially available FO membrane. In these calculations, the salt permeability is set at $B = 10^{-7} \text{ m/s}$, the concentrated solution is seawater (0.55 M) and the dilute solution has a concentration of 5 mM.

currently available membrane parameters and stack design, increased mass transfer offers little to gain – operating at a higher Reynolds number of 100 would increase the power density by $\sim 35\%$. Moreover, if the membrane conductivity were increased by one order of magnitude, the gain in power density would be a meager 11%. This trend is illustrated in Fig. 7, where the power density is plotted against the membrane area conductivity, for different crossflow velocities as well as a ‘complete mixing’ case. A similar trend is observed when the feed channel height is varied, as shown in Fig. 8. An ‘ideal’ RED stack would have a highly ion-conductive membrane and well-mixed streams but would still require a finite channel height for pumping the dilute solution. The results illustrate that changing the channel height has the greatest impact on the power density; with currently available membranes, decreasing the channel height three-fold, from 0.6 mm to 0.2 mm, results in a 2.6-fold increase in the power density.

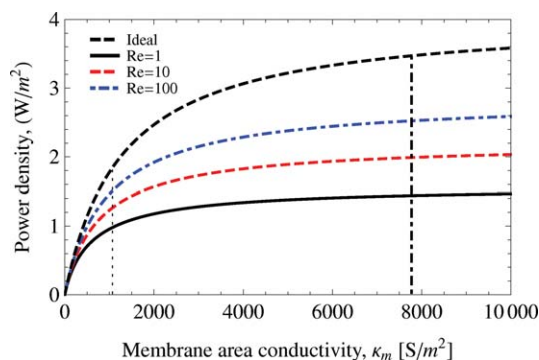


Fig. 7 Variation of RED power density with average membrane area conductivity illustrating the effect of external mixing. Also shown is an ideal power curve, calculated without any mass transfer limitations. The vertical dotted and dash-dotted lines mark the conductivity of commercial heterogeneous and homogeneous membranes, respectively. In these calculations, the average permselectivity is set at $\alpha = 0.95$, the channel height is $h = 200 \mu\text{m}$, the concentrated solution is seawater (0.55 M) and the dilute solution has a concentration of 5 mM.

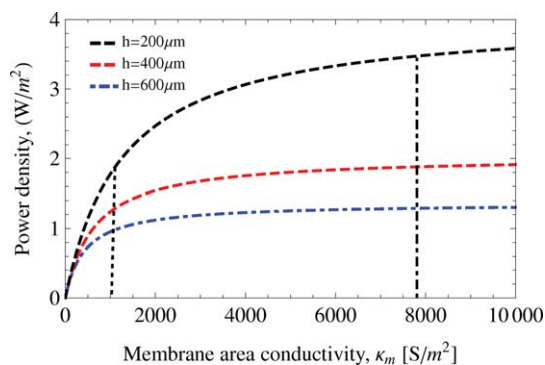


Fig. 8 Variation of RED power density with average membrane area conductivity, illustrating the effect of the feed channel height, h , under complete mixing. The vertical dotted and dash-dotted lines mark the conductivity of commercial heterogeneous and homogeneous membranes, respectively. In these calculations, the average permselectivity is set at $\alpha = 0.95$, the concentrated solution is seawater (0.55 M) and the dilute solution has a concentration of 5 mM.

Membrane selectivity

Salt leakage has been viewed as a significant loss mechanism in PRO, primarily due to the fact that with low salinity feeds the main reason for ICP is salt transport across the membrane from the draw to the feed. This is intimately tied with the structure factor, which is the main parameter controlling the severity of ICP. However, when non-ideal feeds are used the main cause for ICP is salt accumulation and not salt-leakage. Acknowledging this point warrants the consideration of a different paradigm for future development of PRO membranes – the goal is to increase water transport, even if such an increase incurs a concurrent decrease in salt rejection; in other words, *as long as the net outcome is an increased power output*, who cares about salt leakage? Efficiency set aside, the purpose of PRO is power generation, not separation. This point is illustrated in Fig. 9, where the power density is plotted against the membrane permeability, for varying salt permeabilities and structure factors. As may be seen, there is little to be gained when the membrane selectivity is higher than that currently available; in

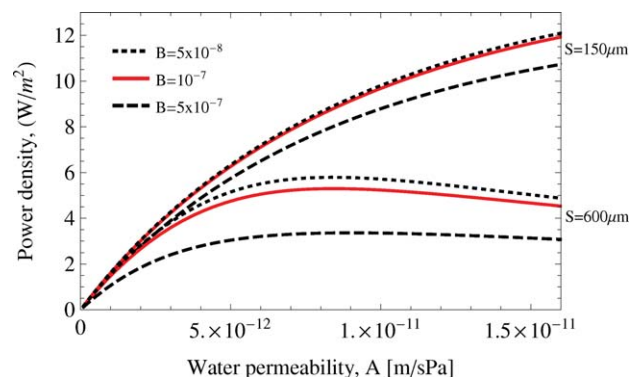


Fig. 9 Variation of PRO power density with increasing water permeability, for different salt permeabilities and structure factors. In these calculations, the Reynolds number is set at $Re = 100$, the concentrated solution is seawater (0.55 M) and the dilute solution has a concentration of 5 mM.

fact, if the structure factor is low (e.g. 150 μm) power output will increase as the membrane permeability is improved, even at the expense of losing selectivity five-fold. This is a major point to consider in future development of PRO membranes, since experience shows that membrane permeability usually comes at some penalty in selectivity.³⁴ Process efficiency will, of course, be reduced since salt leakage represents a loss mechanism; however, it would appear that such losses may be an inevitable consequence of increasing the water permeability. Nevertheless, the power gain would certainly offset the lowered efficiency.

For RED, the permselectivity plays a comparatively more important role since it does not induce losses but in effect controls the transport of charge – the power source itself. Nevertheless, results suggest that this effect is not very significant – increasing the average permselectivity from the currently available value of 0.95 to unity will increase the power density by 9%. If improved membrane conductivity would result in reduced permselectivity (the trade-off between transport resistance and selectivity), these two effects would all but cancel out any improvement to the achieved power output; for example, upon reducing the permselectivity to 0.9, an order of magnitude conductivity increase would result in a 3–15% power gain for a corresponding Reynolds number ranging between ~ 1 –100.

Optimized membrane permeability for PRO

Our PRO simulations have illustrated that, given a set of inherent ‘inefficiencies’, namely the salt permeability, structure factor and external mass transfer coefficient, there exists an optimal membrane permeability, which maximizes power. In light of this important observation, the compilation of membrane characteristics, presented in Table 2, was used to compare performance based on reported values with that achievable with an ‘optimized’ water permeability coefficient. The results are presented in Fig. 10. All the membranes considered, save two, are not at their optimal performance in terms of matching the permeability to all other membrane traits. Moreover, this analysis shows that even membranes with large structure factors (>1 mm) are limited by their permeability, *not the structure factor*.

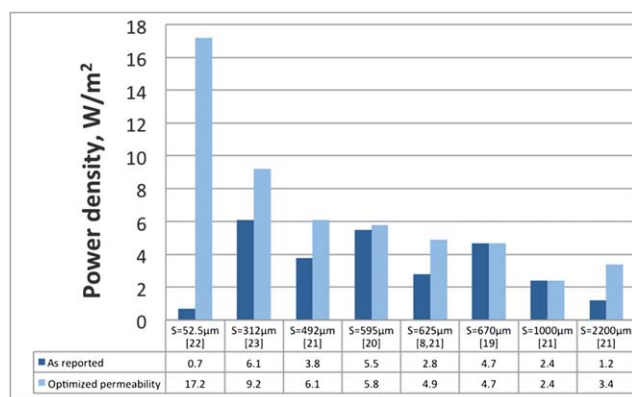


Fig. 10 Calculated PRO power density for membrane properties as reported and with an ‘optimized’ permeability. In these calculations, the Reynolds number is set at $\text{Re} = 100$, the concentrated solution is seawater (0.55 M) and the dilute solution has a concentration of 5 mM.

In fact, the membrane with the smallest structure factor is also the one with the lowest achievable power density, due to its exceedingly low water permeability. Only the membrane with the highest water permeability was actually limited by its structure factor. This is a straightforward illustration of some misconceptions regarding the relative importance of PRO parameters. In particular, it shows that the efforts aimed at reducing the structure factor are of little use if they are not accompanied by increased water permeability, even at the expense of salt rejection.

A comparison of PRO and RED

Finally, we turn to compare the performance of the two membrane-based processes considered. This is done based on the simplified models presented and is made for two scenarios; the first considers process and membrane parameters which are based on the current state-of-the-art as reported in the recent literature (Fig. 11a); the other considers potential improvements (Fig. 11b). The parameters used for both scenarios are listed in Table 4. The main improvements to PRO are in the increased water permeability, with an assumed penalty to the salt rejection, and the decreased structure factor. For RED, an increased conductivity is assumed without a reduction in permselectivity (e.g. a thinner membrane), and the channel height is further reduced.

Note that the RED power density contours exhibit an inflection point at low dilute stream salinity. This is due to the increased resistance of the solution as it approaches the conductivity of pure water, at which point the concentration gradient required to maintain a constant power density increases sharply. The point of inflection itself represents the conditions which conspire to produce the minimum resistance in the dilute channel, through the combined effects of the channel height and solution conductivity, as given in eqn (10). This is an important point to consider, as it may be beneficial for the RED process to operate with slightly brackish water as the dilute stream, resulting in a lowered resistance at reasonable channel heights.

The presented calculations suggest that, based on power density, PRO has a better potential for use as a means for harvesting salinity-gradient energy. This is already true for commercially available membranes, and with potential possible improvements to the membranes the gap becomes even greater, in favor of PRO. This is true no matter what salinity gradient is used as the energy source, in contrast with the conclusions drawn by Post *et al.*³⁵ In their paper from 2007, they provided an insightful comparison of PRO and RED with the conclusion that RED produces a higher power density for low salinity gradients, such as the sea-river water pair. The membrane parameters used in the present study are generally better than those used by Post *et al.*³⁵ for both RED and PRO. Specifically, the commercialization of FO membranes has already made PRO the more promising option, with a much higher potential for future improvement. For example, the current state-of-the-art, optimum power density achievable for PRO for the sea-river water pair is 2.3W/m² compared with 1.3W/m² for RED. With projected improvements, the gap increases to 7.7W/m² vs. 3.4W/m² for the sea-river water pair, while if RO brine is used the corresponding values become 21.2W/m² and 5.2W/m².

It is, however, imperative to note that these results may be misleading if not considered in the context of a full-scale

Table 4 Process characteristics used for calculation of power density

PRO	Water Permeability ($\times 10^{-12}$ m/Pa·s)	Salt Permeability ($\times 10^{-7}$ m/s)	Structure factor (μm)
State of the art	2.2	1.2	625
Projected	10	5	150

RED	Conductivity ($\times 10^4$ S/m ²)	Permselectivity	Channel height (μm)
State of the art	0.8	0.95	200
Projected	3.5	0.95	100

the concentrated stream (the seawater) but also for the diluted stream (river-water), so as to avoid the irreversible clogging of the porous support. Such additional pre-treatment may amount to a considerable added cost.

The situation is seemingly simpler for RED; from a recent economic assessment it may be inferred that the most crucial component for economic viability is the cost of the ion-exchange membranes.⁴ If such membranes were available at a cost of ~ 2.5 $\$/\text{m}^2$, providing a power density of 2 W/m^2 , estimated costs could be as low as $\$4,500/\text{kW}$ installed and $\sim \$0.1/\text{kWh}$,⁴ placing it in a competitive position. However, currently achievable power densities are 25% of this projected value; moreover, ion-exchange membranes are commercially available at prices ranging between $\$100$ – $200/\text{m}^2$, the lower value being representative of heterogeneous membranes. It is quite obvious that incorporating these values into the RED cost analysis would result in significantly higher costs, with installed costs probably at least one order of magnitude higher.

From these estimates it is quite clear that any real prospect for commercialization of either PRO or RED would rely not only on improvements to process efficiency, but primarily on improved system capital expense. An important point to make in favor of such prospects is the sheer size of the potential market; for example, the membrane area required for a medium sized, ~ 100 MW PRO power plant would dwarf all the currently operational RO desalination plants. The market for ion-exchange membranes is smaller still. One may, therefore, argue that costs associated with membranes may be driven down by market forces. Future changes in energy cost structure driving at sustainable production may further make the process economics more appealing.

Conclusions

In this paper, we have presented the fundamental principles governing the operation of two membrane-based methods for the extraction of salinity-gradient energy, a renewable power source that is as yet untapped. Specifically, attention has been given to identifying, quantitatively, the main limiting parameters for each process. Furthermore, it has been shown how improvements to these parameters may affect the resulting power output to varying extents. This kind of information is useful for identifying the more promising and viable directions for research aimed at increasing the efficiency of these processes. In conclusion, the following observations may be made:

1) For RED, very little may be gained by further improving the membranes as the process is ultimately limited by the dilute

channel electrical resistance; therefore, the most promising direction for improvement of RED is in the design of the dilute feed channel. In contrast, PRO membranes have much potential for improvement, with a significant impact on the power production.

2) The most important PRO parameter to be improved is the water permeability; our results show that the membranes available today and, indeed, many of the prototype membranes reported in the literature are not limited by the structure factor but by their permeability.

3) In PRO, decreased salt rejection as a result of improved permeability may be tolerated, *provided that the structure factor is concurrently reduced*.

4) Both processes, particularly RED, require further module-scale design and optimization; flow configurations, mass transfer, viscous dissipation and energy recovery must be considered with the aid of more elaborate mathematical models.

While economic assessments based on current cost estimates and performance are rather bleak, it would seem that potential cost reductions are viable. In fact, it may be concluded that reducing capital equipment costs may be a key factor in the large-scale implementation of these technologies for power production. In particular, development of cheap ion-exchange membranes is a promising avenue for making RED an economically viable option.

List of symbols

A	Water permeability coefficient, $\text{m} \cdot \text{Pa}^{-1} \text{s}^{-1}$
B	Salt permeability coefficient, $\text{m} \cdot \text{s}^{-1}$
c	Concentration, $\text{mole} \cdot \text{m}^{-3}$
d_h	Hydraulic diameter, m
D	Solute diffusion coefficient, $\text{m}^2 \cdot \text{s}^{-1}$
E_{mix}	Energy of mixing, J
F	Faraday constant, $\text{C} \cdot \text{mole}^{-1}$
h	Channel height, m
I	Current, A
J	Ion mass flux, $\text{kg} \cdot \text{s}^{-1}$
J_w	Water flux, $\text{m} \cdot \text{s}^{-1}$
k	Mass transfer coefficient, $\text{m} \cdot \text{s}^{-1}$
P	Pressure, Pa
R	Area resistance, $\text{Ohm} \cdot \text{m}^2$
R_g	Universal gas constant, $\text{J} \cdot \text{mole}^{-1} \cdot \text{K}^{-1}$
Re	Reynolds number, ud_h/ν
S	Structure factor, m
Sc	Schmidt number
T	Absolute temperature, $^\circ\text{K}$
u	Velocity, $\text{m} \cdot \text{s}^{-1}$
V	Volume, m^3 or Electric potential, V
W	Power density, $\text{W} \cdot \text{m}^{-2}$

Greek Letters

α	Permselectivity
δ	Thickness of support layer, m
ε	Porosity

ϕ	Dilution ratio
τ	Tortuosity
π	Osmotic pressure, Pa
ν	Kinematic viscosity, $\text{m}^2 \cdot \text{s}^{-1}$

Subscripts

b	Bulk
c	Concentrated
d	Dilute
m	Membrane

Acknowledgements

GZR was funded by a Vaadia-BARD Postdoctoral Fellowship, Award No. FI-435-2010 from BARD, The United States - Israel Binational Agricultural Research and Development Fund.

Notes and references

- G. L. Wick and W. R. Schmitt, *Mar. Technol. Soc. J.*, 1977, **11**(5–6), 16.
- J. D. Isaacs and R. J. Seymour, The ocean as a power resource, *Int. J. Environ. Stud.*, 1973, **4**(1), 201.
- US energy information administration website, International energy outlook 2010. <http://www.eia.doe.gov/oiaf/ieo/ieoecg.html>.
- J. W. Post, PhD dissertation, 2009, Wageningen University, The Netherlands.
- E. Corcoran, C. Nellemann, E. Baker, R. Bos, D. Osborn and H. Savelli (eds). 2010. Sick Water? The central role of wastewater management in sustainable development. *A Rapid Response Assessment*. United Nations Environment Program, UN-HABITAT, GRID-Arendal. www.grida.no.
- Statkraft website http://www.statkraft.com/Images/Osmotic%20Nov%202009%20ENG_tcm9-11474.pdf.
- R. S. Norman, Water Salination - Source of Energy, *Science*, 1974, **186**, 350.
- S. Loeb, Osmotic Power-Plants, *Science*, 1975, **189**, 654.
- G. D. Mehta and S. Loeb, *J. Membr. Sci.*, 1978, **4**, 261.
- K. L. Lee, R. W. Baker and H. K. Lonsdale, Membranes for power generation by pressure-retarded osmosis, *J. Membr. Sci.*, 1981, **8**, 141.
- A. Achilli, T. Y. Cath and A. E. Childress, *J. Membr. Sci.*, 2009, **343**, 42.
- G. Guillen and E. M. V. Hoek, *Chem. Eng. J.*, 2009, **149**, 221.
- J. N. Weinstein and F. B. Leitz, *Science*, 1976, **191**, 557.
- J. Veerman, R. M. de Jong, M. Saakes, S. J. Metz and G. J. Harmsen, *J. Membr. Sci.*, 2009, **343**, 7.
- P. Dlugolecki, A. Gambier, K. Nijmeijer and M. Wessling, *Environ. Sci. Technol.*, 2009, **43**, 6888.
- P. Dlugolecki, J. Dabrowska, K. Nijmeijer and M. Wessling, *J. Membr. Sci.*, 2010, **347**, 101.
- J. Veerman, M. Saakes, S. J. Metz and G. J. Harmsen, *J. Appl. Electrochem.*, 2010, **40**, 1461.
- J. Veerman, M. Saakes, S. J. Metz and G. J. Harmsen, *Environ. Sci. Technol.*, 2010, **44**, 9207.
- J. W. Post, H. V. M. Hamelers and C. J. N. Buisman, *J. Membr. Sci.*, 2009, **330**, 65.
- G. T. Gray, J. R. McCutcheon and M. Elimelech, *Desalination*, 2006, **197**, 1.
- J. R. McCutcheon and M. Elimelech, *J. Membr. Sci.*, 2006, **284**, 237.
- K. Gerstandt, K. V. Peinemann, S. E. Skilhagen, T. Thorsen and T. Holt, *Desalination*, 2008, **224**, 64.
- L. S. Wang, C. Y. Tang, S. Chou, C. Qiu and A. G. Fane, *J. Membr. Sci.*, 2010, **355**, 158.
- N. Y. Yip, A. Tiraferri, W. A. Phillip, J. D. Schiffman and M. Elimelech, *Environ. Sci. Technol.*, 2010, **44**, 3812.
- S. Zhang, K. Y. Wang, T. S. Chung, H. Chen, Y. C. Jean and G. Amy, *J. Membr. Sci.*, 2010, **360**, 522.
- A. Tiraferri, N. Y. Yip, W. A. Phillip, J. D. Schiffman and M. Elimelech, *J. Membr. Sci.*, 2011, **367**, 340.
- Y. Xu, X. Peng, C. Y. Tang, Q. S. Fu and S. Nie, *J. Membr. Sci.*, 2010, **348**, 298.
- S. E. Skilhagen, J. E. Dugstad and R. J. Aaberg, *Desalination*, 2008, **220**, 476.
- R. E. Pattle, *Nature*, 1954, **174**, 660.
- R. E. Lacey, *Ocean Eng.*, 1980, **7**, 1.
- P. Dlugolecki, K. Nijmeijer, S. Metz and M. Wessling, *J. Membr. Sci.*, 2008, **319**, 214.
- T. W. Xu, *J. Membr. Sci.*, 2005, **263**, 1.
- J. Veerman, M. Saakes, S. J. Metz and G. J. Harmsen, *Chem. Eng. J.*, 2011, **166**, 256.
- G. M. Geise, H. B. Park, A. C. Sagle, B. D. Freeman and J. E. McGrath, *J. Membr. Sci.*, 2011, **369**, 130.
- J. W. Post, J. Veerman, H. V. M. Hamelers, G. J. W. Euverink, S. J. Metz, K. Nijmeijer and C. J. N. Buisman, *J. Membr. Sci.*, 2007, **288**, 218.
- J. Veerman, M. Saakes, S. J. Metz and G. J. Harmsen, *J. Membr. Sci.*, 2009, **327**, 136.
- S. Loeb, *Desalination*, 2002, **143**, 115.